Low threshold current, low resistance 1.3 μm InAs-InGaAs quantum-dot VCSELs with fully doped DBRs grown by MBE

Hsin-Chieh Yu*[a], Jyh-Shyang Wang [b], Yan-Kuin Su [a], Shoou-Jinn Chang [a],
Hao-Chung Kuo [c], Fang-I Lai [c], Y. H. Chang [c], and Hong-Pin D. Yang [d]
[a]Advanced Optoelectronics Technology Center and Institute of Microelectronics,
National Cheng Kung University, No.1, University Rd. Tainan 70101, Taiwan;
[b] Department of Physics, Chung Yuan Christian University.
No. 200, Chung Pei Rd., Chung Li 32023, Taiwan;
[c] Institute of Electro-Optical Engineering, National Chiao Tung University,
No. 1001 Ta Hsueh Road, Hsinchu 300, Taiwan;
[d] Opto-Electronics & Systems Laboratories, Industrial Technology Research Institute,
No. 195 Chung Hsing Rd., Sec.4 Chu Tung, Hsinchu 310, Taiwan.

ABSTRACT

The processing technology of 1.3μm InAs-InGaAs quantum-dot VCSELs with fully doped DBRs grown by MBE will be demonstrated. The threshold currents of the fabricated devices with 10 μm oxide-confined aperture are 0.7mA, which correspond to 890A/cm^2 threshold current density. And the threshold voltage of the device is 1.03V and maximum output power is 33 μW. The series resistance is 85 Ω which is 10 times lower then our preliminary work and 3 times lower then intracavity contacted InAs-InGaAs quantum-dot VCSEL. This relatively lower resistance can even comparable with the best result reported in InGaAs oxide-confined VCSELs with intracavity contact.

Keywords: 1.3 μm, InAs-InGaAs, quantum dot, VCSEL, fully doped DBR, MBE.

1. INTRODUCTION

THE development of GaAs-based vertical-cavity surface-emitting lasers (VCSELs) emitting in the 1.3μm range remains a fruitful area of laser diode research, offering significant growth and fabrication challenges but also a large variety of possible epitaxial material combinations to investigate. Recently reported results on GaAs-based laser diodes (LDs) and VCSELs emitting near 1.3 μm include devices composed of GaAsSb/GaAs [1], [2] and InGaAsN/GaAs [3]-[5] with multiple quantum well (MQW) active regions. Additionally, the combination of GaAsSb and InGaAsN forms a GaInNAsSb-GaAs heterostructure that may lase at 1.3 μm [6]. Also of note is highly strained InGaAs QWs which provide optical gain at wavelengths at or near 1.3 μm [7], [8]. In contrast to QWs, self-assembled InAs/InGaAs quantum dots (QDs) can be used to fabricate 1.3 μm GaAs-based LDs and VCSELs [9], [10]. Oxide-confined (OC-) VCSELs, wherein lateral oxidation is used to form current and optical confinement apertures, need to be etched to expose the high Al composition AlGaAs layer close to the active region. This etching process will result in a non-planar surface that complicates one or two subsequent lift-off metallization steps. The most common physical geometries for OC-VCSEL fabrication are the intracavity metal contacted structure [10] and the mesa structure planarized by a spin-on glass or polyimide, benzocyclobutene (BCB) etc. [7, 11]. However, the etching process required to form mesas for the placement of intracavity contacts is extremely critical to device performance and it is difficult to accurately control during fabrication. During each of two mesa fabrication steps, the etching depth must be controlled to stop exactly on the thin, heavily doped contact layers adjacent to the microcavity. The etching process tolerance is typically too small to obtain a high yield, even if the etch is performed with *in situ* reflectance monitoring. The resultant non-planar configuration complicates the subsequent metallization process. Typically the intracavity contacting method is used for MBE-grown VCSEL fabrication [10], because the DBRs are commonly undoped to avoid free carrier absorption and the need to compositionally grade the DBR heterointerfaces. As a result, the device yields of intracavity contacted OC-VCSELs are lower.

*q1889113@nckualumni.org.tw; phone 886-6-2757575-62382; fax 886-6-2356226

Vertical-Cavity Surface-Emitting Lasers XI, edited by Kent D. Choquette, James K. Guenter,
Proc. of SPIE Vol. 6484, 64840E, (2007) · 0277-786X/07/$18 · doi: 10.1117/12.697732

In this paper we report a near-planar processing method for InAs QD OCVCSELs that is expected to be readily adaptable to a high volume production line with high device yields and state-of-the-art QD VCSEL performance. With this fabrication technique, we herein demonstrate GaAs-based QD VCSELs that operate continuous wave (CW) at room temperature (RT) with peak output powers exceeding 33 μW. The threshold current and threshold voltage are 0.7mA and 1.03V, respectively. It is also worth to note that the series resistance is about 85 Ω, which is comparable with the best reported result by using intracavity contacts.

2. EXPERIMENTS

The InAs QD OC-VCSEL wafers used in the experiments were prepared by NL Nanosemiconductor GmbH (Germany) using solid-source molecular beam epitaxy (MBE) and grown on an (001)-oriented n-GaAs substrate. The active region consists 9 sheets of InAs pyramidal islands formed by a 2 monolayer-thick InAs deposition, and embedded in an 8 nm-thick $In_{0.15}Ga_{0.85}As$ QW overgrowth layer separated by 30 nm-thick GaAs barrier layers. The 9 sheets of InAs/InGaAs QDs are divided into 3 groups and each group consists of 3 closely-spaced sheets of dots. For the purpose of placing all the three groups of QD layers exactly at antinode positions of the resonant standing wave field to obtain higher optical gain, the microcavity optical length is elongated to 2λ to sustain at least three normalized squared electric-field antinode positions inside the microcavity.

The n- and p-doped DBRs are composed of λ/4-thick $GaAs/Al_{0.9}Ga_{0.1}As$ layers with digital interface grading to help reduce each VCSEL's series resistance. The n- and p-doped DBRs consisted of 33.5 and 27 periods, respectively, and the calculated reflectance *R* for each mirror greater than 0.99. The DBR material layers are δ-doped with Si at N_D ~$5x10^{18}$ cm^{-3} and with C at N_A~$5x10^{18}$ cm^{-3} adjacent to the digitally graded interfaces, respectively. The doping level of each DBR periods was reduced to about $2x10^{17}$ cm^{-3} for the purpose of reducing free carrier absorption. A 20 nm-thick AlAs layer was placed at the interface between the first p-DBR quarter-wave layer and the microcavity active region. This AlAs layer is later selectively oxidized in water vapor to serve as both a current and wave-guiding aperture. A schematic illustration of a fabricated QD VCSEL is given in Fig. 1(a).

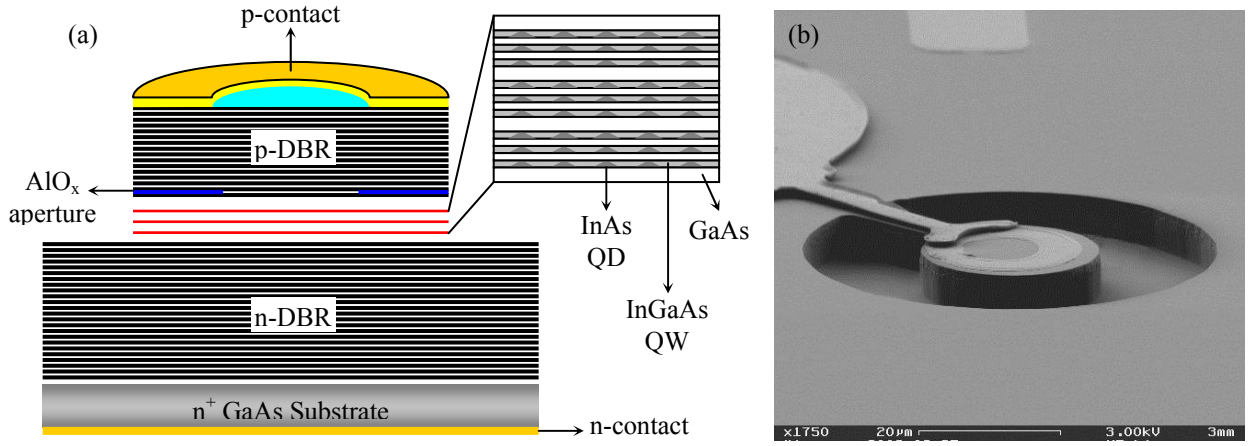

Fig. 1. (a) Schematic illustration of the oxide-confined QD VCSEL with fully doped DBRs grown by MBE. The 2λ -thick active region consists of 9 sheets of InAs QDs embedded in 8 nm-thick InGaAs QWs. (b) Scanning electron microscope (SEM) photograph of the fabricated device.

After MBE growth, a 1.7 μm-thick SiN_x layer was deposited onto the wafer sample surface by plasma enhanced chemical vapor deposition (PECVD) at 300°C. This SiN_x layer was used as a hard mask for a subsequent dry etching step. Conventional photolithography and reactive ion etching (RIE) with *in situ* reflectance monitoring were then performed to define a mesa pattern on the SiN_x. Trenched mesa etching was then performed using RIE to transfer the pattern of the SiN_x hard mask onto the wafer sample. The shape of the trench is not a thick-line letter "O" (i.e. an annulus) but rather a thick-line letter "C" that is almost a closed circle, as shown in Fig. 1(b). The etched depth of the trench was carefully controlled to expose the 20 nm-thick AlAs layer. The total etching depth was is 6.5 μm. Selective wet oxidation wasthen preformed at 400°C in steam. The mesa diameter of the oxidized VCSELs was 22 μm with a 12

μm oxide aperture. After the removal of the residual SiN_x, we used PECVD to deposit a 150 nm-thick SiO_2 layer onto the wafer samples for device passivation. This passivation layer was then partially etched for contact window formation. Subsequently Ti (30 nm) / Pt (50 nm) / Au (200 nm) was deposited onto the topmost heavily doped (N_A~$2x10^{19}$ cm^{-3}) p^+-GaAs to serve as p-contact metal. After substrate lapping down to 200 μm, AuGe (50 nm) / Ni (20 nm) / Au (350 nm) was deposited onto the backside of the samples to serve as the n-contact metal. The processing technique and resultant device appearance is almost identical to the MOVPE grown 850 nm OC-VCSEL we previously reported [12], except the trenched mesa etching for our QD VCSELs is deeper. Note that our process includes neither the intracavity contacts nor the polyimide planarization.

2.1 InAs quantum-dot VCSEL with Zn difussion

Initially the measured light output power (L) from the QD VCSEL was lower than expected because the power reflectance (R) of the top DBR was quite high. Therefore we removed the top three periods of the p-DBR (including the p^+-GaAs contact layer) to slightly reduce the reflectivity and fabricated a new set of devices. As a result, the top and bottom DBRs then consisted of 24 and 33.5 periods, respectively. To compensate for the reduce doping in the topmost p-DBR layer after the etching of the DBR, we first performed a Zn diffusion at 570°C for 8 minutes across the entire wafer sample surface in an As_4 overpressure prior to device fabrication. The shallow Zn diffusion serves to reconstruct the p^+-GaAs topmost ohmic contact layer.

2.2 Proton implantation of InAs quantum-dot VCSEL

To improve the high-speed modulation performance of our QD VCSELs, we implanted protons to decrease the parasitic capacitance [13]. Protons were implanted at energies of 200, 300, and 400 keV with a dose of $5x10^{14}$ cm^{-2} at each of these energies. The implanted aperture lay over the oxide aperture and the diameter is also 12 μm. According to the stopping and range of ions in matter (SRIM) simulation results, the peak implant depth is about 3.57 μm from the surface to keep from damaging the active region.

2.3 InAs quantum-dot VCSEL without Zn difussion

The additional Zn diffusion makes the process more complicated and decreases the yield. Moreover the Zn diffusion also increases absorptive and scattering losses. Hence another sample consists 33.5 and 25 pairs of n- and p-doped DBRs, respectively, was processed. By using the digital grading interfaces in doped DBRs and optimal doping profile, the poor thermal conductivity of $Al_{0.9}Ga_{0.1}As$ alloys was improved. As a result the relatively small thermal resistance should also be achieved at the same time [14]. The processing method and device appearance is identical to the devices with Zn diffusion mentioned above, except the composition of the oxide layer varied from AlAs to $Al_{0.98}Ga_{0.02}As$. Since the pair number of top DBR was reduced to 25, it is unnecessary to remove the upmost heavily doped p^+ contact layer. And subsequently the additional Zn diffusion can be avoided.

3. RESULTS AND DISCUSSION

The measured continuous wave (CW), room temperature (RT) light output power (L) and applied voltage (V) versus current (I) characteristic of one of our typical QD VCSELs with Zn diffusion is given in Fig. 2 (a). The mesa diameter is 22 μm and the trench width is 15 μm. The internal diameter of the VCSEL's top metal ring contact is 10 μm and the bonding pad diameter is 85 μm, respectively. The large bonding pad connects directly to the VCSEL's top metal ring contact by lying flush on the wafer surface and across the section of the trench that is not etched. Thus, our process does not require the formation of an air-bridge.

3.1 DC characteristics of InAs-InGaAs quantum-dot VCSEL with Zn diffusion

As extracted from the data in Fig. 2(a), the turn-on voltage of the fabricated device is 1.26 V, the threshold voltage (V_{th}) is 6.9 V, and the threshold current (I_{th}) is about 1.7 mA. Since the circular current aperture diameter is 12 μm, the corresponding threshold current density is $1.5kA/cm^2$. The maximum output power is 0.33mW with a differential slope efficiency of 0.23 W/A. Our devices exhibit large series resistance of about 0.8 to 1.3 kΩ within the operational range, which is approximately 4 times larger than previously reported QD VCSELs with intracavity metal contacts [15]. We attribute this large series resistance to significant current heating due to unoptimized DBR interface grading and Zn diffusion conditions. Moreover, this additional Zn diffusion increases absorptive and scattering losses. These device losses conspire to cause an early rollover in the L-I curve and thus serve to limit the peak output power. The lasing

spectrum of the fabricated device at a drive current of 3.2 mA is shown in Fig. 2(b). The peak lasing wavelength is 1.275 μm.

As expected, this peak emission wavelength is coincident with the peak emission wavelength of our previously reported resonant cavity light emitting diodes (RCLEDs) containing similar active regions [16]. It is clear from the data in Fig. 2(b) that the fabricated QD VCSELs operate in a single mode with a side-mode suppression ratio (SMSR) of 28 dB and a full-width-at-half-maximum (FWHM) of 0.24 nm.

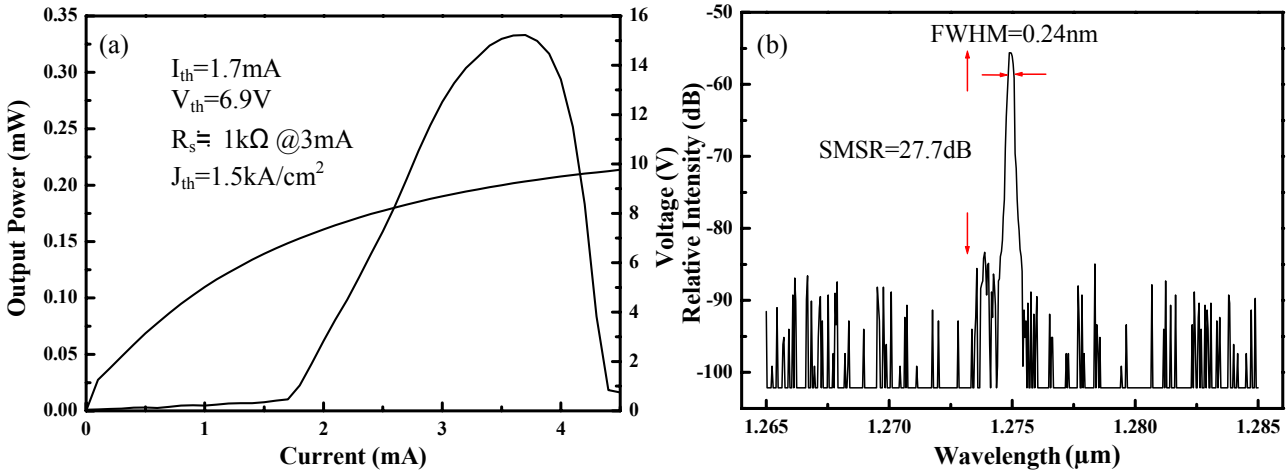

Fig. 2. (a) L-I-V characteristics of the InAs QD VCSEL with Zn diffusion. The turn-on voltage is 1.26 V and I_{th} is 1.7 mA with 0.33 mW maximum output power. (b) Lasing spectrum of the InAs QD VCSEL with 3.2 mA drive current shows the peak wavelength is 1.275 μm and SMSR is 28 dB.

3.2 Modulation response of InAs-InGaAs quantum-dot VCSEL

The measured modulation response of the implanted QD OC-VCSEL at several bias currents from 2.0 to 3.2 mA is shown in Fig. 3. The 3 dB frequency (f_{3dB}) at a bias current of 2.6 mA is 2 GHz.

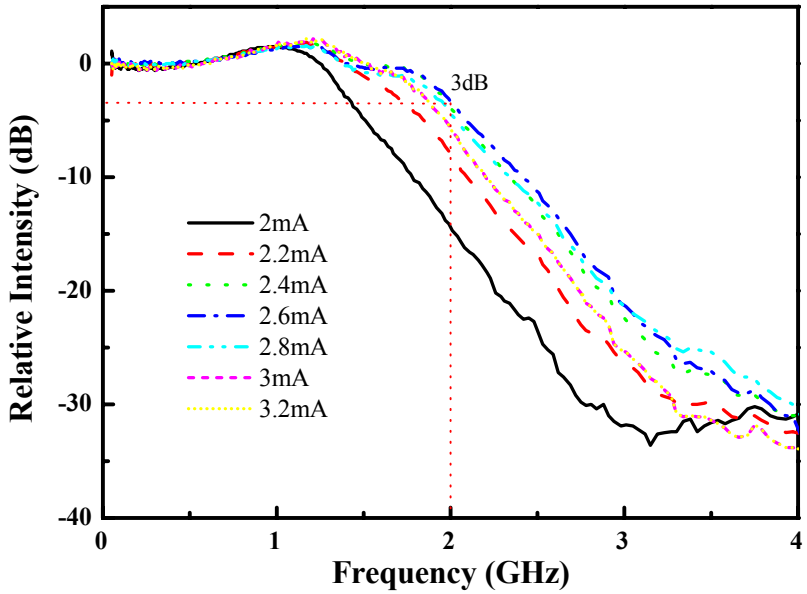

Fig. 3. Modulation response of the InAs QD VCSEL with additional proton implantation. The maximum 3dB modulation bandwidth is 2 GHz.

Figure 4 is a plot of the 3 dB frequency versus $(I–I_{th})^{1/2}$. From the slope of the data in Fig. 4, the modulation current efficiency factor (MCEF) can be extracted. The MECF is constant at about 2.5 GHz/$(mA)^{1/2}$ for current drive currents between about 1.7 to 2.6 mA. These results indicate that our QD OC-VCSELs have great potential to be modulated at data rates up to 2.5 Giga-bit per second (Gb/s) and thus our devices should meet the OC-48 standard.

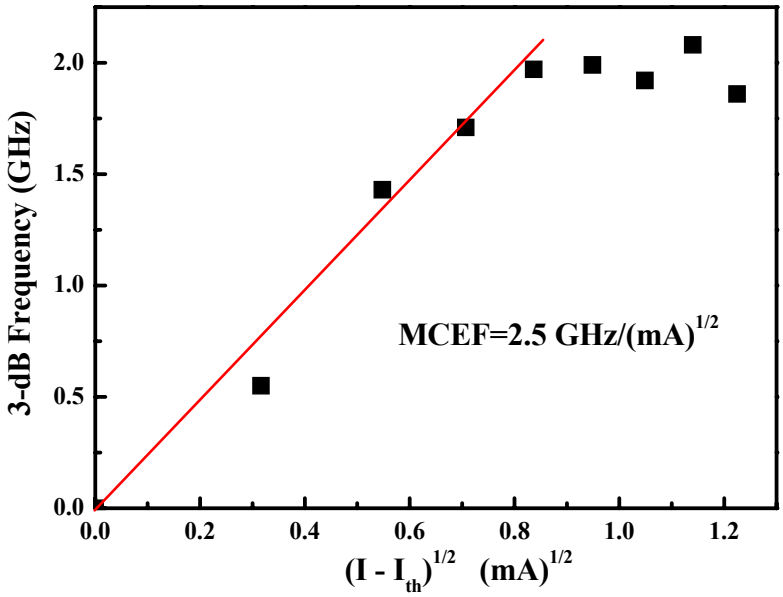

Fig. 4. Modulation current efficiency factor (MCEF) of the fabricated device with additional implantation is 2.5 GHz/$(mA)^{1/2}$.

The eye diagrams shown in Fig. 5 represent the fabricated device was modulated at 1.25 and 2.5 Gb/s . The implanted InAs QD VCSEL shows a clear and symmetrical eye diagram at 1.25 Gb/s. At 2.5 Gb/s, the eye was degraded due to the overshoot and insufficient bandwidth. The relatively lower modulation frequency compared with our previous work [13] can be ascribed to the large series resistance. Larger series resistance and parasitic capacitance means large time constant, and consequently limit the modulation speed. In order to improve the modulation characteristics, further reducing the series resistance is necessary.

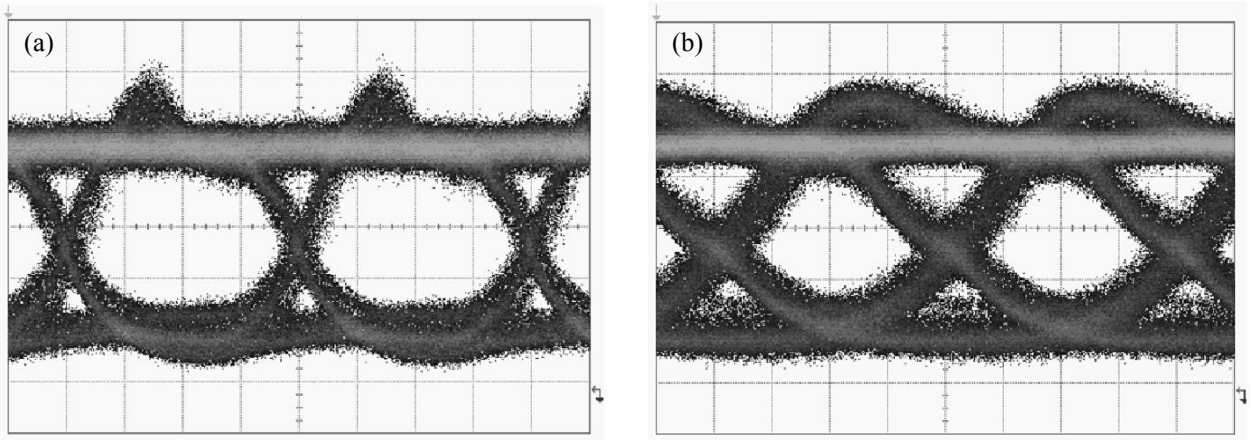

Fig. 5. Eye diagram of the QD VCSELs with proton implantation at (a) 1.25 and (b) 2.5 Gb/s (time scale was 200 and 100 ps/div).

3.3 DC characteristics of InAs-InGaAs quantum-dot VCSEL without Zn diffusion

As revealed in Fig. 6(a), the threshold voltage (V_{th}) of the fabricated device without Zn diffusion is 1.03 V, and the threshold current (I_{th}) is about 0.7 mA. Since the circular current aperture diameter is 10 μm, the corresponding threshold current density (J_{th}) is 890kA/cm^2. The maximum output power is 33 μW and series resistance is about 85Ω within the operational range, which is approximately 10 times lower than that of QD VCSELs with Zn diffusion. The resistance is also 3 times lower than InAs-InGaAs QD VCSELs with intracavity metal contacts emitting in 1.3 μm range [15]. And this relatively lower resistance can even comparable with the lowest record of 80Ω reported in InGaAs quantum well VCSEL with intracavity contact emitting in 980nm range [17]. The lasing spectrum in Fig. 6(b) shows the peak wavelength of the fabricated QD VCSELs is 1.274 μm with 5mA driving current. These devices can also be operated in a single mode with a side-mode suppression ratio (SMSR) of 20 dB and a full-width-at-half-maximum (FWHM) of 0.4 nm.

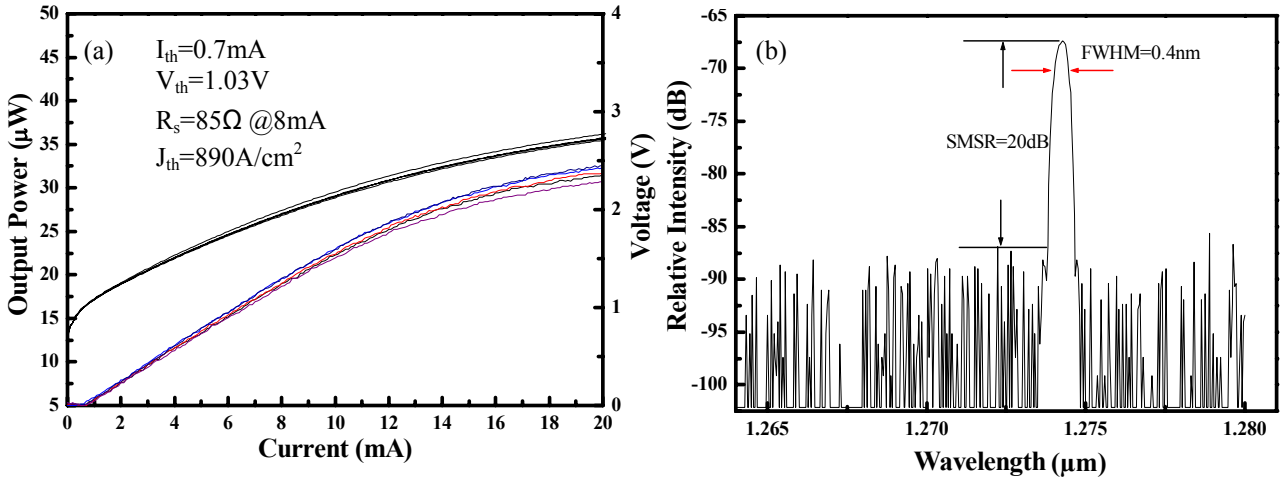

Fig. 6. (a) L-I-V characteristics of the InAs QD VCSEL. The I_{th} is 1.7 mA and V_{th} is 1.03V with 33 μW maximum output power. (b) Lasing spectrum of the InAs QD VCSEL with 5 mA drive current shows the peak wavelength is 1.274 μm and SMSR is 20 dB.

By using the digital grading interfaces in doped DBRs and optimal doping profile, the poor thermal conductivity of $Al_{0.9}Ga_{0.1}As$ alloys was improved. As a result the relatively small thermal resistance is achieved, which makes the fabricated device can be driven up to 20mA. It is very promising for the fabricated device to be modulated at higher speed because of the low resistance. But the reflectivity of top DBR is still too high to extract more output power, it is very difficult to measure the modulation response and eye diagram.

4. CONCLUSSION

The 1.3μ m InAs-InGaAs quantum-dot VCSELs with fully doped DBRs grown by MBE were fabricated. The threshold current and voltage of the fabricated devices with 10 μm oxide-confined aperture are 0.7mA and 1.03V, respectively. And the corresponding threshold current density is 890A/cm^2. The device can be driven up to 20mA and maximum output power is 33 μW. The series resistance is 85Ω which is 3 times lower then intracavity contacted InAs-InGaAs quantum-dot VCSEL, and comparable with the best result reported in InGaAs oxide-confined VCSELs with intracavity contact. Slightly reducing the reflectivity of top DBR shall increase the output power, and the modulation response can also be further improved.

ACKNOWLEDGEMENTS

The authors would like to thank Dr. A. R. Kovsh and Dr. S. S. Mikhrin of the NL-Nanosemiconductor GmbH for their assistance and cooperation in epitaxial growth.

REFERENCES

1. F. Quochi, D. C. Kilper, J. E. Cunningham, M. Dinu, J. Shah, "Continuous-wave operation of a 1.3-μm GaAsSb-GaAs quantum-well vertical-cavity surface-emitting laser at room temperature," *IEEE Photon. Technol. Lett.*, , vol. 13, pp.921-923, 2001.
2. T. Anan, M. Yamada, K. Nishi, K. Kurihara, K. Tokutome, A. Kamei and S. Sugou, "Continuous-wave operation of 1.30μm GaAsSb/GaAs VCSELs," *Electron. Lett.*, vol.37, pp.566-567, 2001.
3. M. Kondow, T. Kitatani, S. Nakatsuka, M. C. Larson, K. Nakahara, Y. Yazawa, M. Okai and K. Uomi, "GaInNAs: a novel material for long-wavelength semiconductor lasers," *IEEE J. Select. Topics. Quantum. Electron.*, vol. 3 , pp. 719-730, 1997.
4. K. D. Choquette, J. F. Klem, A. J. Fischer, O. Blum, A. A. Allerman, I. J. Fritz, S. R. Kurtz, W. G. Breiland, R. Sieg, K. M. Geib, J. W. Scott, R. L. Naone, "Room temperature continuous wave InGaAsN quantum well vertical-cavity lasers emitting at 1.3 μm," *Electron. Lett.* , vol.36 , pp.1388-1390, 2000.
5. T. Takeuchi, Y. L. Chang, M. Leary, A. Tandon, H. C. Luan, D. Bour, S. Corzine, R. Twist, M. Tan, "1.3 μm InGaAsN vertical cavity surface emitting lasers grown by MOCVD," *Electron. Lett.* , vol. 38 , pp.1438-1440, 2002.
6. H. Shimizu, C. Setiagung, M. Ariga, Y. Ikenaga, K. Kumada, T. Hama, N. Ueda, N. Iwai, and A. Kasukawa, "1.3-μm-Range GaInNAsSb–GaAs VCSELs," *IEEE J. Select. Topics. Quantum. Electron.*, vol. 9 , pp. 1214-1219, 2003.
7. C. Asplund, P. Sundgren, S. Mogg, M. Hammar, U. Christiansson, V. Oscarsson, C. Runnstrm, E. Ödling, J. Malmquist, "1260 nm InGaAs vertical-cavity lasers," *Electron. Lett.* , vol.38, pp.635-636, 2002.
8. P. Sundgren, R. Marcks von Würtemberg, J. Berggren, M. Hammar, M. Ghisoni, V. Oscarsson, E. Ödling and J. Malmquist, "High-performance 1.3 μ m InGaAs vertical cavity surface emitting lasers," *Electron. Lett.*, vol. 39, pp. 1128-1129, 2003.
9. D. L. Huffaker, G. Park, Z. Zou, O. B. Shchekin and D. G. Deppe, "Continuous-wave low-threshold performance of 1.3 μm InGaAs-GaAs quantum-dot lasers," *IEEE J. Select. Topics. Quantum. Electron.*, vol. 6,pp. 452-461, 2000.
10. J. A. Lott, N. N. Ledentsov, V. M. Ustinov, N. A. Maleev, A. E. Zhukov, A. R. Kovsh, M. V. Maximov, B. V. Volovik, Z. I. Alferov and D. Bimberg, "InAs-InGaAs quantum dot VCSELs on GaAs substrates emitting at 1.3 μm," *Electron. Lett.*, vol. 36, pp. 1384-1385, 2000.
11. N. AL-Omari, and K. L. Lear, "Polyimide-Planarized Vertical-Cavity Surface-Emitting Lasers With 17.0-GHz Bandwidth," *IEEE Photon. Technol. Lett.*, vol. 16, pp.969-971, 2004.
12. H. C. Yu, S. J. Chang, Y. K. Su, C. P. Sung, Y. W. Lin, H. P. Yang, C. Y. Huang, J. M. Wang, "A simple method for fabrication of high speed vertical cavity surface emitting lasers," *Materials Sci. Eng.: B*, v.106, pp.101-104, 2004.
13. H. C. Yu, S. J. Chang, Y. K. Su, C. P. Sung, H. P. Yang, C. Y. Huang, Y. W. Lin, J. M. Wang, F. I. Lai and H. C. Kuo, "Improvement of High-Speed Oxide-Confined Vertical-Cavity Surface-Emitting Lasers," *Jpn. J. Appl. Phys.*, v.43, pp.1947-1950, 2004.

14. Sergey A. Blokhin, Nikolai A. Maleev, Alexander G. Kuzmenkov, Alexey V. Sakharov, Marina M. Kulagina, Yuri M. Shernyakov, Innokenty I. Novikov, Mikhail V. Maximov, Victor M. Ustinov, Alexey R. Kovsh, Sergey S. Mikhrin, Nikolai N. Ledentsov, Gray Lin, and Jim Y. Chi, "Vertical-Cavity Surface-Emitting Lasers Based on Submonolayer InGaAs Quantum Dots," *IEEE J. Quantum. Electron.*, vol. 42 , pp. 851-858, 2006.

15. V. M. Ustinov, A. E. Zhukov, A. Y. Egorov, N. A. Maleev, "*Quantum Dot Lasers*," Oxford University Press, pp. 260-263, 2003.

16. Y. K. Su, H. C. Yu, S. J. Chang, C. T. Lee, J. S. Wang, A. R. Kovsh, Y. T. Wu, K. F. Lin, C. Y. Huang, "1.3 μm InAs quantum dot resonant cavity light emitting diodes," *Materials Sci Eng.: B*, v.110, pp. 256-259, 2004.

17. Michael H. MacDougal, Jon Geske, Chao-Kun Lin, Aaron E. Bond, and P. Daniel Dapkus, "Low Resistance Intracavity-Contacted Oxide-Aperture VCSEL's," *IEEE Photon. Technol. Lett.*, vol. 10, pp.9-11, 1998.